PMT measurements in Antares

A.Creusot[a], O.Kalekin[b,*], V.Kulikovskiy[c], Ya.Yakovenko[d], on behalf of the ANTARES collaboration

[a] *APC, 10, rue Alice Domon et Lonie Duquet,75205 Paris, France*
[b] *ECAP, Erwin-Rommel-Str. 1, 91058 Erlangen, Germany*
[c] *INFN Genova, Via Dodecaneso 33, 16146 Genova, Italy*
[d] *Moscow State University , Leninskie Gori,119991 Moscow, Russia*

Abstract

The comparison of simulated and real data in the Antares experiment shows some discrepancies. Differences are observed in the charge distribution of background hits, in the trigger efficiency, and in the counting rate of ^{40}K decay induced events. These discrepancies must be understood to improve data analysis. It turns out that most of the simulated/real data mismatch can be explained by a undetailed description of the PMT response in the simulations. PMT parameters such as late pulses, afterpulses and angular acceptance have been reviewed and when necessary measurements of these parameters have been carried out using Antares PMTs and optical modules. In addition a more detailed simulation of the angular acceptance of the Antares optical module has been performed. Results of these studies are presented.

Keywords: Antares, neutrino telescope, optical module, photomultiplier tube, PMT
2000 MSC: 95.55.Vj, 95.85.Ry, 85.60.Ha

1. Introduction

ANTARES is an underwater neutrino telescope at 2500 m depth in the Mediterranean Sea, 40 km off the shore of Toulon. The experiment aims to detect high energy cosmic neutrinos using a 3D array of 900 photomultipliers [1]. The ANTARES detector is composed of 12 strings anchored on the seabed and pulled up by a buoy. A string is 480m long, it consists of an anchor and 25 storeys. The storey comprises 3 optical modules (OMs) each one made of a 17" glass sphere housing a 10" HAMAMATSU photomultiplier tube (PMT), looking downwards at 45 degrees to the vertical. The experiment delivers data since March 2006, when the first line was connected. Since May 2008 the ANTARES telescope is fully operational. The large amount of collected data allowed a detailed comparison of these data with respect to the simulated ones. Some discrepancies were found in the charge distribution of the background hits (experimental data have a much longer tail at large amplitudes), in trigger efficiency, and in the observed counting rate of ^{40}K induced events. Most parts of these mismatches can be explained by an oversimplified description of the PMTs and of the OMs in simulations. To obtain a more precise description of these detector components, a series of new measurements on the PMTs and OMs have started in Antares. In the first part of the paper we report on the angular acceptance of Antares optical modules while the measurement of the PMT parameters such as late and after pulses is presented in the second part.

2. Angular acceptance

2.1. Scan of OM surface

Scans using a light emitting diode (LED) with maximum intensity centred at 470 nm were performed on two available OMs at the Erlangen Centre for Astroparticle Physics (ECAP). OMs were scanned using a goniometer-scanner in a few direction across OM's centre of symmetry with steps of 2 degrees. LED pulses of 20 ns long were delivered to the OM surface via optical fibre. For each scan point, at least 10,000 pulses were collected. The light beam of ∼1 mm diameter was always perpendicular to the OM surface. OM response signals were digitized using analogue-to-digital converter (ADC) CAMAC's module LeCroy 2249A.

Signal amplitude was changed from a few tens of photoelectrons (phe) down to ∼1 phe for different points of scans. The following analysis procedure was then applied to the scan data. The number of photoelectrons (phe) at each point of the scan was assumed to be Poisson distributed P(n;μ), where μ is the average number of phe per pulse. The charge distribution of the single phe was approximated by a Gaussian function with parameters Q_1 - mean charge, and σ_1. Parameters of n-phe charge distribution were calculated as follow: $Q_n = n{\cdot}Q_1$, $\sigma_n^2 = n{\cdot}\sigma_1^2+\sigma_0^2$, where σ_0 is obtained from the pedestal distribution fitted with the Gauss function. This parameter characterises the electronics noise. Small amplitude signals (see Fig. 1) were

*Corresponding author
Email address: kalekin@physik.uni-erlangen.de (O.Kalekin)

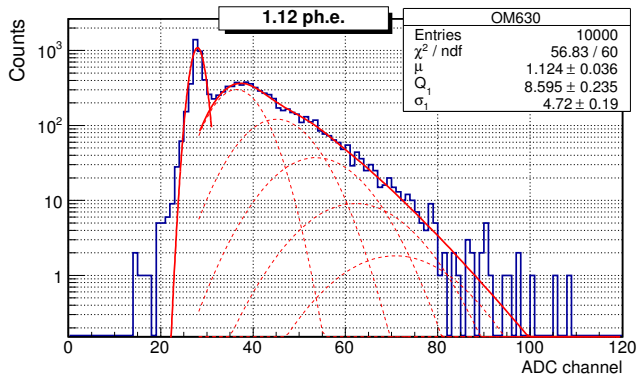

Figure 1: Fit of the optical module signal response for large angle and correspondently small amplitude.

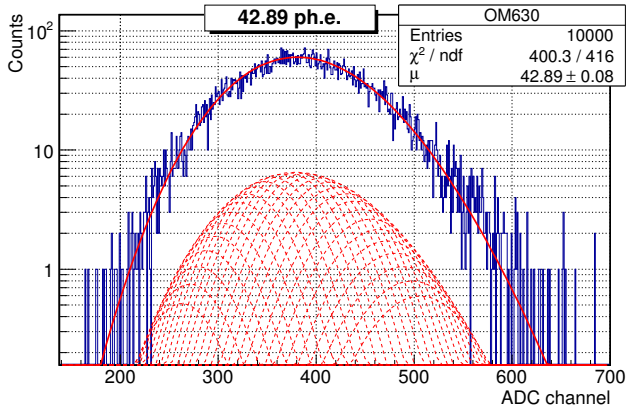

Figure 2: Fit of the optical module signal response for small angle and correspondently large amplitude. Single photoelectron parameters are fixed.

fitted by a combination of the above described Poisson and Gauss functions with free parameters μ, Q_1, and σ_1. For large amplitude signals (see Figure 2), parameters Q_1 and σ_1 were taken from the small amplitude signal fit and fixed.

The values of the mean number of phe obtained for each point were normalised to the point at -10 degrees from the centre. An example of the resulting scan distribution is shown in Figure 3. The large depletion at the centre is caused by a badly transparent spot in the glass in this particular OM. A few small depletions at -25°, -15°, and 22° are produced by the shadows of the μ-metal cage surrounding the PMT to shield the magnetic field of the Earth. The same Figure shows that the light beam misses the PMT's photocathode at angles -48° and 45°. The increase of the signal at larger angles is due to the internal reflection towards the photocathode of the light at the gel-air surface. The asymmetry of the presented distribution is caused by a non-homogeneous detection efficiency of the PMT over the photocathode surface. The radial scans on the OMs were used in dedicated Geant 4 simulations of the Antares OM. In these simulations, the photodetection efficiency of the PMT over the photocathode area was tuned to fit the

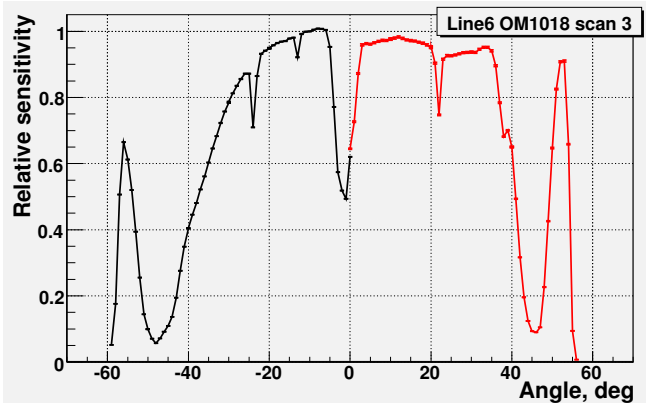

Figure 3: Radial scan of the Antares optical module at ECAP

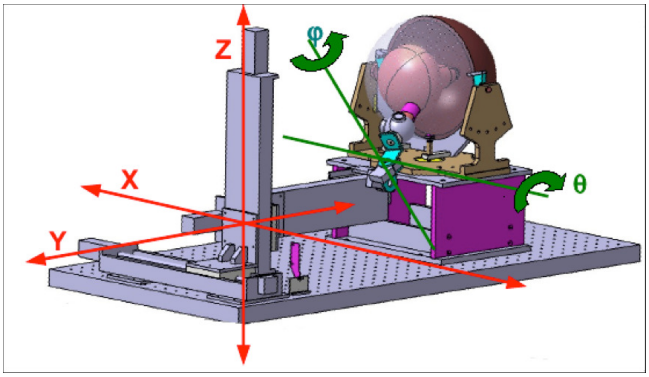

Figure 4: Scanner at APC with an OM

experimental OM radial scans. Then, the OM angular acceptance was obtained simulating the OM response to a parallel light beam in water illuminating the whole OM at different inclinations angles. The resulting angular acceptance curve is presented in Figure 8 as dashed line.

The goniometer used for these measurements had only one automated degree of freedom. For this reason, a full scan measurement was time consuming and the scanning of the whole OM surface was almost impossible. The full surface scan could provide much more accurate information for the simulations. Therefore, an upgrade of the scanner has been recently done at ECAP with the extension at 3 automated degrees of freedom. An even more advanced scanner has been developed at the AstroParticule et Cosmologie (APC) laboratory in Paris. The design of the scanner with 5 degrees of freedom is presented in Figure 4. This setup allows to scan the whole OM surface with any inclination of the light beam. The first detailed sensitivity map of the Antares OM is presented in Figure 5. A radial scan of the Antares optical module is presented in Figure 6.

2.2. Angular acceptance in water

The test bench at ECAP is equipped with a large water tank (see Figure 7) which was used for measurements

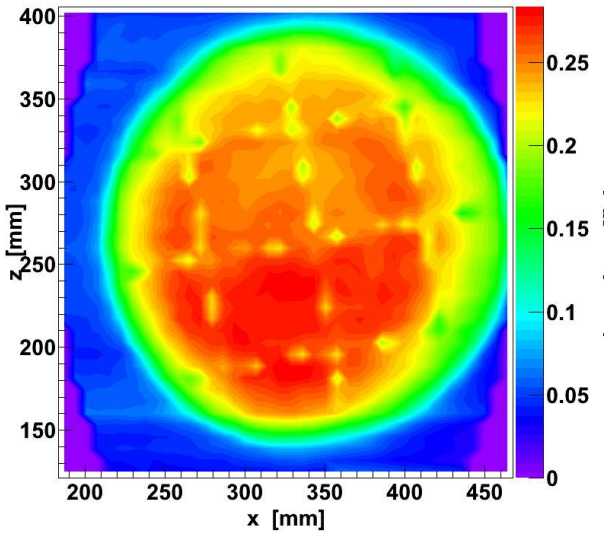

Figure 5: Scan of the whole surface of the Antares optical module at APC. Colors indicate OM's sensitivity in arbitrary units

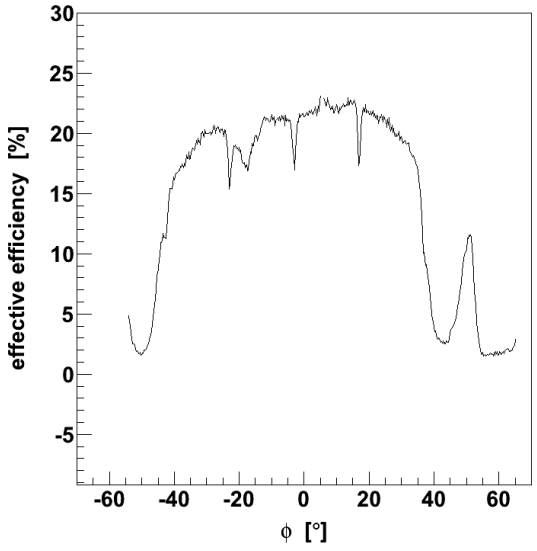

Figure 6: Radial scan of the Antares optical module at APC. Photon detection efficiency (y-axis) was obtained using NIST calibrated photodiode.

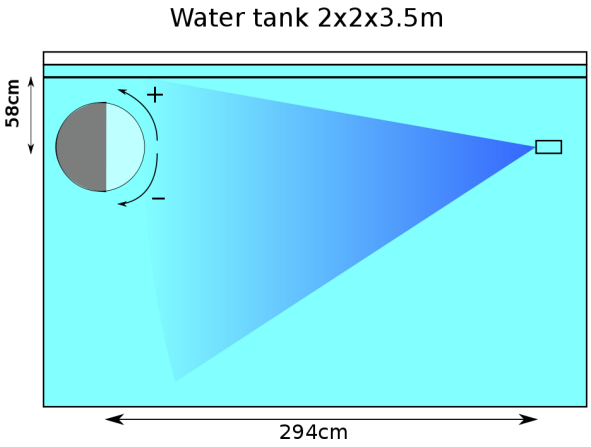

Figure 7: Drawing of the OM angular acceptance measurements in water tank

of the angular acceptance of the Antares OMs in tap water. The OM was deployed ∼60 cm under water. The OM holder allows the OM rotation in a vertical plane in the range of ±180° with steps of 0.36°. In the presented measurements, the scan range was ±129.6° with steps of 5.4°. At the opposite side of the tank, an LED sealed into a gel bulb was set up. A light diffuser was glued to the side of the bulb faced towards the OM while the other sides were covered with a black neoprene. The same type of LED (470 nm) as for the surface scans was used. The LED was driven with 20 ns electric pulses at a frequency of 1 kHz. Small non-rotating neoprene walls were used on the sides of the OM to reject scattered light from the sides. A black plastic film was placed a few centimetres under water to prevent internal reflections of light from the surface and to protect from outside light. The same read-out as described in Section 2.1 was used while the intensity of the light source was adjusted to detect 30-40 phe per pulse for the front illuminated OM. For the largest angles, 0.3-0.5 phe per pulse was detected. The same analysis method as in Section 2.1 was applied to the obtained data.

The results of scans of two OMs are presented in Figure 8 as solid lines. There, the angular acceptance obtained from simulations with Geant 4 is shown as a dashed line. In principle, the simulated and experimental curves should be identical. For large angles (cos(A)<-0.5), the differences can be ascribed to the presence of scattered light in the measurements, as confirmed by the flattering of the curves. In addition, the detected signal for these angles was below 1 phe. Therefore, for future measurements in a water tank, a more careful protection from scattered light should be taken. Differences in the middle range of angles (-0.5<cos(A)<0.6) are to be understood. They can originate from both sides – from simulations, because of limited input from radial surface scans of OMs, and from measurements, because of presence of scattered light.

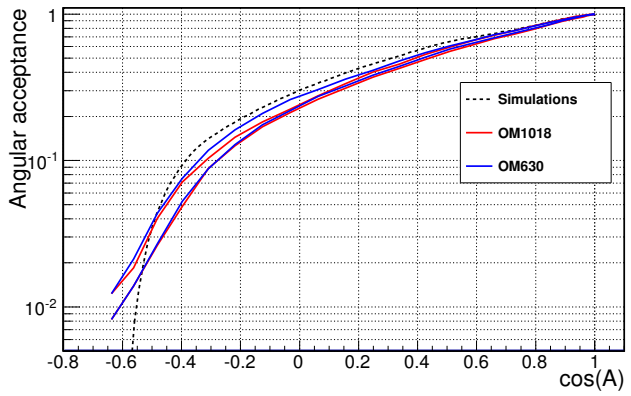

Figure 8: Angular acceptance of the Antares optical module.

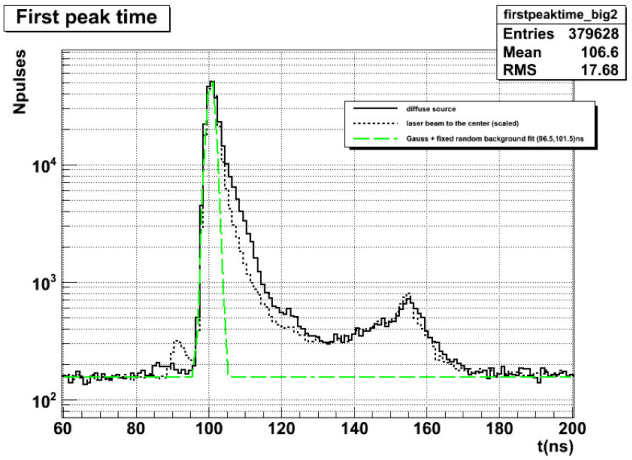

Figure 9: Time distribution of detected pulses for the Hamamatsu 10-inch R7081 PMT. Solid line – all pulses for the uniform illuminated PMT. Dashed line (long dashes) – gauss fit of the main peak. Dashed line (short dashes) – all pulses for the PMT illuminated at centre.

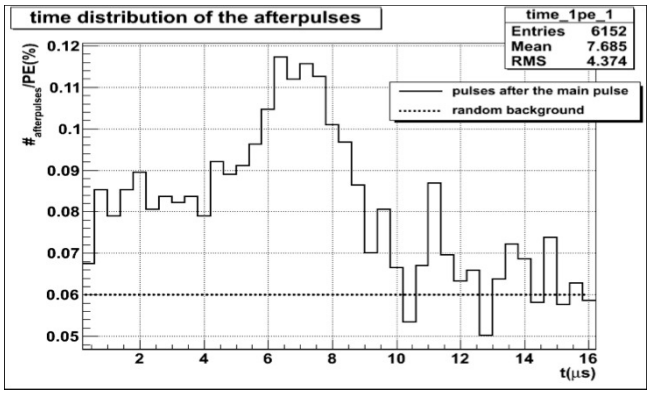

Figure 10: Observed distribution of late afterpulses in a time range of $0.5 - 9\mu s$ with a high peak at $\sim 7\mu s$ for the Hamamatsu 10-inch R7081 PMT.

3. Afterpulses

The measurements of the afterpulses on a 10-inch R7081 PMT of Antares were performed in the INFN Laboratory in Genova. A laser with 439 nm wavelength and pulse duration of a few ps was used as a light source. Illumination level was ∼0.01 phe/pulse to produce on average one signal at the PMT anode every 500 light pulses sent by the laser. The output of the PMT anode was sent to a fast, 1GHz, CAEN digitizer V1731 in coincidence with the Laser SYNC out. Signals with amplitude higher than 10 mV were sampled in a predefined time window synchronized with laser pulses. This window can be as long as 16 μs.

The time distribution of these single phe PMT pulses with respect to the laser is presented in Figure 9 as a solid line. The main peak of the distribution at a fixed electronic delay of 100 ns is followed by late pulses up to 150 ns. Hits before the main pulses and after the late pulses are dark noise pulses. Late pulses can be caused by photoelectrones elastically scattered on the first dynode and accelerated back by the electric field or by photons ejected from dynodes by electrons and arriving at the photocathode. In some cases, these are observed in a presence of the main pulse. If so, such pulses are identified as fast afterpulses. When the main peak is fitted by a gaussian on a flat background dark noise, the amount of late pulses is equal to 28% of all detected hits. Usually, only the broad main peak of the one phe transit time distribution (TT) of the PMT is used in simulations to describe the full PMT's timing response. However, this is not enough for an adequate description of a PMT. The use of the shown late pulse distribution in simulations can increase their quality and solve discrepancies in trigger efficiency and counting rate of ^{40}K background events.

Another observed type of afterpulses is presented in Figure 10. These afterpulses are caused by atoms/molecules of the residual gases ionised by the photoelectrons which drift towards the photocathode. The typical arrival time of these afterpulses is a few microseconds. Therefore, they are called "late afterpulses". The total amount of late afterpulses in the measured PMT is 0.8% of the detected main hits. Late afterpulses have very broad and relatively flat charge distribution achieving values of more than 10 phe. This fact explains the observed long tail of large charge hits in experimental Antares data, which was not taking into account the distribution of afterpulses in the earlier simulations.

4. Acknowledgements

The authors acknowledge the financial support of the funding agencies: Agence Nationale de la Recherche: project ANR-08-JCJC-0061-01, in France; Bundesministerium für Bildung und Forschung (BMBF), in Germany; Istituto Nazionale di Fisica Nucleare, in Italy.

[1] ANTARES Collaboration, A deep sea telescope for high energy neutrinos, *Preprint* arXiv:astro-ph/9907432v1